RISØ

Risø-R-1484(EN)

Predicting formation enthalpies of metal hydrides

Anders Andreasen

Risø National Laboratory
Roskilde
Denmark
December 2004

Risø-R Report

Author: Anders Andreasen
Title: **Predicting formation enthalpies of metal hydrides**
Department: AFM

Risø-R-1484(EN)
December 2004

Abstract:

In order for the hydrogen based society viz. a society in which hydrogen is the primary energy carrier to become realizable an efficient way of storing hydrogen is required. For this purpose metal hydrides are serious candidates. Metal hydrides are formed by chemical reaction between hydrogen and metal and for the stable hydrides this is associated with release of heat (ΔH_f). The more thermodynamically stable the hydride, the larger ΔH_f, and the higher temperature is needed in order to desorp hydrogen (reverse reaction) and vice versa. For practical application the temperature needed for desorption should not be too high i.e. ΔH_f should not be too large. If hydrogen desorption is to be possible below 100^{o}C (which is the ultimate goal if hydrogen storage in metal hydrides should be used in conjunction with a PEM fuel cell), ΔH_f should not exceed -48 kJ/mol. Until recently only intermetallic metal hydrides with a storage capacity less than 2 wt.% H_2 have met this criterion. However, discovering reversible hydrogen storage in complex metal hydrides such as $NaAlH_4$ (5.5 wt. % reversible hydrogen capacity) have revealed a new group of potential candiates. However, still many combination of elements from the periodic table are yet to be explored. Since experimental determination of thermodynamic properties of the vast combinations of elements is tedious it may be advantagous to have a predictive tool for this task. In this report different ways of predicting ΔH_f for binary and ternary metal hydrides are reviewed. Main focus will be on how well these methods perform numerically i.e. how well experimental results are resembled by the model. The theoretical background of the different methods is only briefly reviewed.

ISSN 0106-2840
ISBN 87-550-3382-2

Contract no.:

Group's own reg. no.:

Sponsorship:

Cover :

Pages: 33
Tables: 5
Figures: 16
References: 54

Risø National Laboratory
Information Service Department
P.O.Box 49
DK-4000 Roskilde
Denmark
Telephone +45 46774004
bibl@risoe.dk
Fax +45 46774013
www.risoe.dk

Risø–R–1484(EN)

Predicting formation enthalpies of metal hydrides

Anders Andreasen

Risø National Laboratory, Roskilde, Denmark
October 2004

Abstract In order for the *hydrogen based society* viz. a society in which hydrogen is the primary energy carrier to become realizable an efficient way of storing hydrogen is required. For this purpose metal hydrides are serious candidates. Metal hydrides are formed by chemical reaction between hydrogen and metal and for the stable hydrides this is associated with release of heat (ΔH_f). The more thermodynamically stable the hydride, the larger ΔH_f, and the higher temperature is needed in order to desorb hydrogen (reverse reaction) and vice versa. For practical application the temperature needed for desorption should not be too high i.e. ΔH_f should not be too large. If hydrogen desorption is to be possible below 100 °C (which is the ultimate goal if hydrogen storage in metal hydrides should be used in conjunction with a PEM fuel cell), ΔH_f should not exceed -48 kJ/mol. Until recently only intermetallic metal hydrides with a storage capacity less than 2 wt.% H_2 have met this criterion. However, discovering reversible hydrogen storage in complex metal hydrides such as $NaAlH_4$ (5.5 wt. % reversible hydrogen capacity) have revealed a new group of potential candiates. However, still many combination of elements from the periodic table are yet to be explored. Since experimental determination of thermodynamic properties of the vast combinations of elements is tedious it may be advantagous to have a predictive tool for this task. In this report different ways of predicting ΔH_f for binary and ternary metal hydrides are reviewed. Main focus will be on how well these methods perform numerically i.e. how well experimental results are resembled by the model. The theoretical background of the different methods is only briefly reviewed.

ISBN 87–550–3382–2 (Internet)
ISSN 0106–2840

Print: Pitney Bowes Management Services Denmark A/S · 2004

Contents

1 Introduction

1.1 Towards the hydrogen based society

A growing interest in the transformation of the hydrocarbon based society into a hydrogen based society is emerging around the world. This is induced by the fact that hydrogen offer some key advantages compared to hydrocarbons: Produced by electrolysis of water using renewable energy sources e.g. solar, wind or water power as a source of electricity the need for hydrocarbons is greatly reduced. Further, converting the chemically stored energy in H_2 to electricity in a fuel cell under the right conditions water is the only combustion product.

However, for the hydrocarbon based society to become realizable a suitable way of storing hydrogen in between the production and the use of hydrogen must be offered. This is indeed a problem that needs special attention if hydrogen should become the future choice of energy carrier in mobile applications e.g. cars due to the very specific demands for safety, volumetric energy density, gravimetric energy density etc. [1]. Different ways of storing hydrogen exist e.g storage in high pressure cylinders, storage as liquid hydrogen, physisorption in carbon nanotubes and storage in metal hydrides [2]. In our view the storage of hydrogen in metal hydrides is perhaps the most interesting and challenging [3].

1.2 Hydrogen storage in metals

Storage of hydrogen in metal hydrides is possible since many metals react readily with hydrogen forming a stable metal hydride. For instance, Mg reacts with hydrogen forming a hydride of the form MgH_2. Thus, storing 7.6 wt. % of hydrogen and thereby fulfilling the gravimetric hydrogen density criterion suggested by the U.S. Department of Energy for year 2010 [4]. However, in order to release hydrogen at a pressure of 1 bar the hydride must be heated to above 280 °C. This is because magnesium forms a (too) stable hydride with a heat of formation of approx. ΔH_f=-75 kJ/mol. A car driven by a PEM fuel cell operated at around 80-100 °C is not capable of supplying the required heat for this operation (in fact 100 °C is the upper operable temperature limit for metal hydrides suggested by USDOE [4]). Alternatively, the hydride bed may be heated by combustion of hydrogen. This will however lower the efficiency by approx. 25 % [2]. Another way around this problem is to use another hydride matarial with improved thermodynamical properties e.g. $LaNi_5$ or FeTi which deliver hydrogen at tempeartures as low as 12 °C and -8 °C, respectively. These materials do however fail to meet the gravimetric energy density criterion since they store only 1.5 wt. % and 1.85 wt. % of hydrogen, respectively [5]. To the best of our knowledge no material have been found with properties fulfilling both the energy density criterion and the thermodynamic criterion. So the search continues and new combinations of metals in intermetallic compounds are proposed, prepared and tested experimentally for their hydrogen storage properties. But how do we propose new materials for synthesis with the desired thermodynamic properties? One method is trial-and-error e.g. making slight modifications of a compound with known properties. However, this is indeed a tedious and time consuming approach. Another way is by prediction of the desired properties by calculation either from empirical knowledge or from first principle.

1.3 Outline

In this report different ways of predicting hydride formation enthalpies are evaluated. A number of different approaches will analyzed ranging from simple models such as *Born-Haber cycle*, the *Miedema model* to more advanced methods like *Effective Medium Theory* and *Density Functional Theory*. This report is neither intended as a step-by-step guide for performing these calculations nor is it intended as a detailed description of the theoretical basis of the different models. The main goal is to review the results of the different approaches. The organization of this report is the following: In section 2 we will describe the use of experimentally determined Pressure Composition Isotherms as a tool for deriving thermodynamic parameters. In section 3 a number of different ways of predicting the formation enthalpy of binary metal hydrides will be discussed ranging from empirical/semi-empirical methods to non-empirical methods. In section 4 we expand the picture to account for prediction of formation enthalpies of ternary metal hydrides. The review of methods of predicting the hydride formation enthalpy is by no means intended to give a complete overview of available methods. For instance known methods e.g. the correlation between interstitial hole size and thermodynamic properties of intermetallic compounds proposed by Lundin et al. [6] and the band structure model proposed by Greissen et al. [7] are excluded.

2 Thermodynamic properties from experiments

2.1 The Pressure Composition Isotherm

The Pressure Composition Isotherm from now on called PCI is the work horse when it comes to determination of several key properties of metal hydrides. A generic PCI is depicted in figure 1 (left). When initially increasing the hydrogen pressure at isothermal conditions the adsorbed amount of hydrogen (H/M is the hydrogen to metal stoichiometric ratio) will increase only slightly. This corresponds to the formation of a solid solution of hydrogen and this is denoted the α-phase. When the maximum solubility of hydrogen in the α-phase is reached the hydride phase (β-phase) will start forming. Increasing the hydrogen pressure further will now result in a substantial increase in the absorbed amount of hydrogen. This phenomenon may be explained from the Gibbs phase rule [8]

$$F = 2 - \pi + N \tag{1}$$

where F is the degree of freedom, π is the number of phases and N is the number of chemical species. Thus, the addition of one additional phase is counterbalanced by the loss of a degree of freedom. The pressure at which this transformation takes place is referred to as the plateau pressure and in this region the α-phase and β-phase co-exist. When the stoichiometric hydride have formed completely depleting the β-phase one additional degree of freedom is regained and the additional absorption of hydrogen will now require a huge pressure increase. This corresponds to the solid solution of hydrogen in the β-phase. The plateau pressure gives us valuable information about reversible storage capacity from the width of the plateau and the position of the plateau at a given temperature may give an idea of the stability of the hydride. Stable hydrides ($\Delta H_f << 0$) will require higher temperatures than less stable hydrides ($\Delta H_f < 0$) to reach a certain plateau pressure. Making series of PCI's at different temperatures it is even possible to construct a phase diagram from the end points of the plateaus in the individual PCI's. This

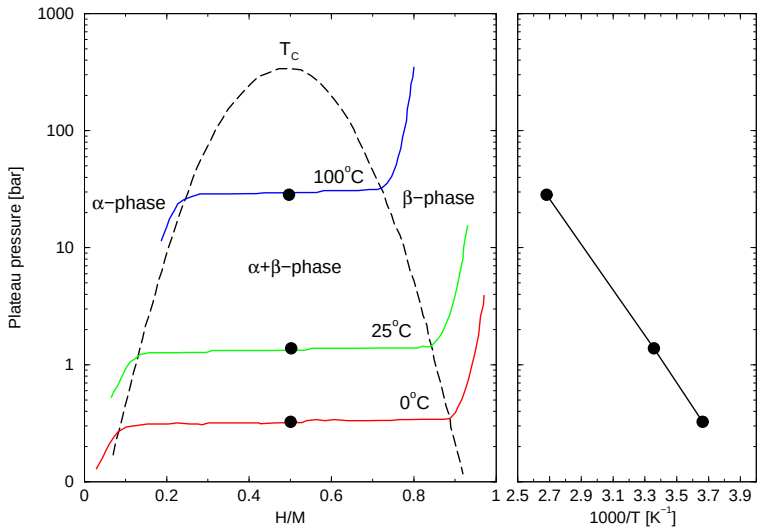

Figure 1. Left: Pressure-Composition-Isotherms (PCI) for a hypothetical metal hydride. Adapted from ref. [1]. Right: Van't Hoff plot for a hypothetical metal hydride derived from the measured pressures at plateau midpoints from the PCI's.

is shown by the dashed line in figure 1.

2.2 Thermodynamic properties from PCI

At the midpoint of the plateau the following equilibrium is assumed to exist between gas phase hydrogen + pure metal and the β-phase to exist:

$$H_2(g) + Me_{pure}(s) \rightleftharpoons Me_\beta(s) \tag{2}$$

thus assuming the amount of hydrogen dissolved in the metal lattice to be negligible. At equilibrium the reaction quotient Q equals the equilibrium constant K.

$$K = \prod_i (\hat{a}_i)^{\nu_i} \tag{3}$$

where $\hat{a}_i$ is the activity coefficient of species i and ν_i is the stoichiometric coefficient of species i. Substituting from eq. 2 assuming the ideal gas description to be valid i.e. $\hat{a}_{H_2} = p_{H_2}/p^\ominus$ where $p^\ominus$ is the thermodynamic reference pressure and assuming that $\hat{a}_{Me_{pure}} = \hat{a}_{Me_\beta} = 1$ we get

$$K^{-1} = \frac{p_{H_2}}{p^\ominus} \tag{4}$$

From the definition of the equilibrium constant we know that $-RT \ln K = \Delta G^\ominus$, where $\Delta G^\ominus$ is the change in standard Gibbs free energy upon hydrogenation. Further the definition of $\Delta G^\ominus = \Delta H^\ominus - T\Delta S^\ominus$ inserted into the equation above yields

$$\ln\left(\frac{p_{H_2}}{p^\ominus}\right) = \frac{\Delta H^\ominus}{RT} - \frac{\Delta S^\ominus}{R} \tag{5}$$

where $\Delta H^\ominus$ and $\Delta S^\ominus$ is the change in standard enthalpy and the change in standard entropy, respectively from now on denoted ΔH_f and ΔS_f. Eq. 5 is known as the Van't Hoff equation and it states that plateau pressure midpoints measured at different temperatures will lie on a straight line when plotted as $\ln(p_{H_2}/p^\ominus)$ vs. reciprocal temperature with slope equal to ΔH_f and intercept ΔS_f cf. figure 1 (right). Hence, from a number of measurements of plateau pressures at different temperatures the Van't Hoff equation can by applied to determine ΔH_f and ΔS_f.

In figure 2 real PCI's are shown for $LaNi_5$ determined at 3 temperatures both for hydrogenation and dehydrogenation, respectively. The PCI clearly demonstrates that for real systems hysteresis and sloping plateaus also comes into play. However this is beyond the scope of the present work. Also shown is the derived Van't Hoff plot. From this ΔH_f for hydrogenation of $LaNi_5H_x$ is found to be equal to -31.1 kJ/mol H_2 in agreement with the literature [9].

2.3 The entropy relationship

If ΔS_f is known *a priori* one single PCI is enough to determine ΔH_f. In fact, it turns out that it is possible to give a reasonable estimate of ΔS_f. In figure 3 the formation enthalpy of a number of different metal hydrides both binary and ternary compounds is plotted against the temperature required to give a plateau pressure of 1 bar H_2. Rearranging eq. 5 with $p_{H_2}/p^\ominus = 1$ gives

$$\Delta H_f = \Delta S_f T \tag{6}$$

Hence, if the entropy change upon hydrogenation is more or less the same regardless of the host metal a plot of the formation enthalpy vs. plateau temperature at 1 bar H_2 should lie on a straight line with slope ΔS_f . According to fig. 3 this is

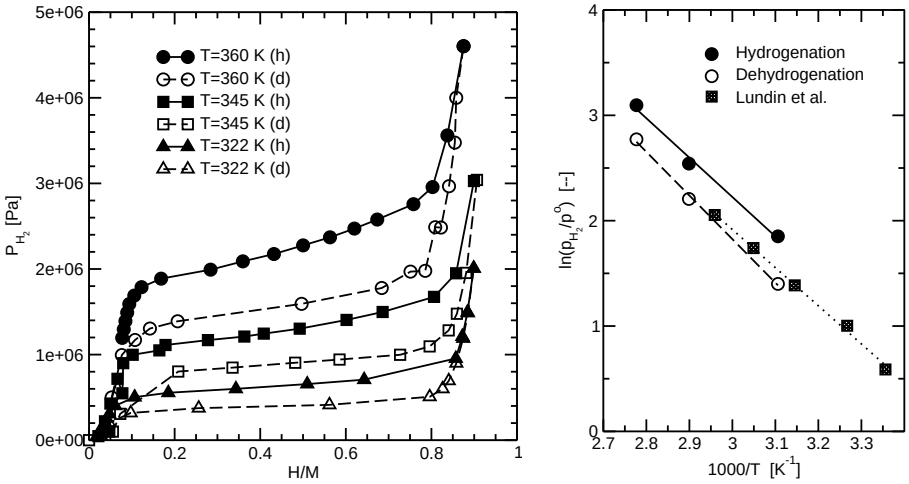

Figure 2. Left: Pressure-Composition-Isotherms (PCI) for $LaNi_5$. Right: Van't Hoff plot measured pressures at plateau midpoints (H/M=0.5) from the PCI's. The Van't Hoff plot of Lundin et al. is from ref. [9]. PCI measurements where performed on a high pressure balance described in detail elsewhere [10].

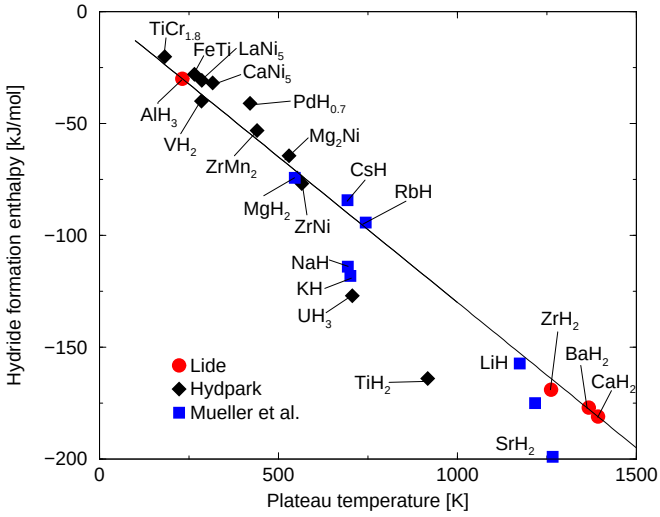

Figure 3. Hydride formation enthalpy, ΔH_f per mole H_2 as a function of the plateau temperature at 1 bar. The plateau temperature is calculated from reported thermodynamic parameters using the Van't Hoff equation. Data represented by circles is from ref. [11], data represented by squares is taken from ref. [12] and data represented by diamonds is taken from ref. [5].

actually the case. The straight line depicted in the figure has slope $\Delta S_f = -130$ J/(mol K). The entropy loss of 130 J/(mol K) roughly corresponds to the loss of the translational degree of freedom when H_2 from the gas phase is absorbed in the metal[1].

As stated earlier the USDOE criterion regarding thermodynamics for a hydrogen storage material is desorption of hydrogen above 1 bar to be possible below 100 °C

[1] A back-on-the envelope calculation using statistical thermodynamics of the translational contribution to the overall entropy using $S = R\ln(Q) + RT\left(\frac{d\ln(Q)}{dT}\right)_V$ where Q is the translational partition function gives 116 J/(mol K).

[4]. Eq. 6 can now be applied to reformulate this criterion in terms of ΔH_f. We find that in order for a metal hydride to meet the USDOE criterion ΔH_f should not be more exothermic than 48 kJ/mol.

3 Binary hydrides

3.1 Born-Haber calculations

The Born-Haber cycle is often applied as a textbook example of evaluating the formation enthalpies of ionic crystals. The formation of a binary hydride can be described by the following overall reaction

$$Me(s) + \frac{n}{2}H_2(g) \rightleftharpoons MeH_n(s) \tag{7}$$

The heat of formation of the metal hydride, ΔH_f, can be determined from calorimetric experiments or derived from PCI-measurements. However, if these experiments are unavailable we may derive it by constructing a Born-Haber thermodynamic cycle as shown in figure 4.

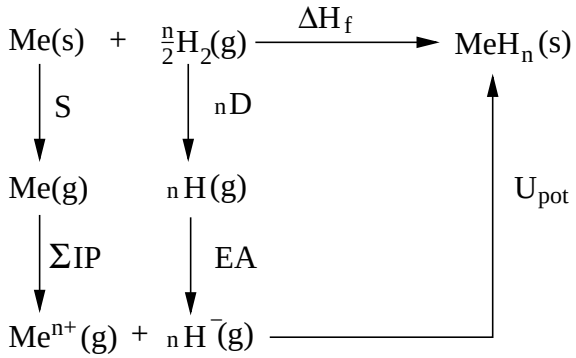

Figure 4. Born-Haber cycle for the formation of solid binary metal hydride from solid metal and gaseous hydrogen

Applying Hess' Law ΔH_f is expressed by

$$\Delta H_f = S + \frac{n}{2}D + \sum_n IP + EA + U_{tot} \tag{8}$$

where S is the sublimation enthalpy of the metal ion i.e. the energy required transfer the solid metal to gaseous form, D is the dissociation enthalpy of the hydrogen molecule, IP is the ionization potential of the metal ion, EA is the electron affinity of the hydrogen atom and U_{tot} is the lattice enthalpy of the metal hydride. The summation of the ionization potential is required for polyvalent metal cations e.g. the total ionization potential of Mg is the summation of the 1. and 2. ionization potential (formation of Mg^+ from Mg^0 and subsequently formation of Mg^{2+} from Mg^+). From above we see that if all terms on the right hand side of eq. 8 is known ΔH_f can be estimated. Tabulated values of S, D, IP and EA can be found in ref. [11].

The total crystal lattice energy U_{tot} when the ions are at their equilibrium positions can be estimated using the *Born-Landé* equation [13].

$$U_{tot} = -\frac{N_A A z_+ z_- e^2}{4\pi\epsilon_0 R_0}\left(1 - \frac{1}{n}\right) \tag{9}$$

where N_A is the Avogadro number, A is the Madelung constant, z_+ and z_- is the number charge of the cation and anion, respectively, e is the electron charge, ϵ_0 is the permittivity in vacuum, R_0 is the shortest separation between cation and anion centers and n is a repulsion coefficient.

Metal hydride	S	$\sum_n IP$	U_{tot}	ΔH_f
LiH	160	520	-920	-96
NaH	108	496	-808	-60
KH	90	419	-714	-61
RbH	81	403	-685	-57
CsH	79	376	-644	-45
MgH_2	147	2177	-2791	-104
CaH_2	178	1726	-2410	-144
SrH_2	164	1605	-2250	-119
BaH_2	180	1461	-2121	-118
ScH_3	378	4235	-5439	-237
TiH_2	473	1959	-2866	-72
VH	514	648	-1184	122
CrH	396	650	-1050	140
FeH_3	416	5255	-5724	536
NiH	430	733	-929	378
CuH	337	742	-828	395
ZnH_2	130	2626	-2870	249
LaH_2	431	1597	-2380	10
CeH_2	423	1573	-2414	-56
PrH_2	356	1537	-2448	-193
NdH_2	328	1560	-2464	-214

Table 1. Parameters used in the Born-Haber cycle calculations and calculated ΔH_f for selected alkali metal hydrides, alkaline earth metal hydrides, transition metal hydrides and rare earth hydrides. All listed values are given in kJ/mol. Calculated values for U_{tot} have been adapted from ref. [11].

We have used the Born-Haber cycle to predict the formation enthalpy of a number of binary hydrides based on alkali metals, alkaline earth metals, transition metals and rare earth metals. The calculational parameters are summarized in table 1. Also listed are the predicted values of ΔH_f.

Predicted ΔH_f are compared with experimentally determined values in figure 5. As shown on the figure predicted values of the formation enthalpy for the alkali metal hydrides are in excellent agreement with experiments taken the simplicity of the model into account. This is not surprising due to the ionic like bonding in the alkali metal hydrides. The alkaline earth metal hydrides are less ionic in nature (the difference in electronegativity between the metal cation and the hydrogen anion is less than for the alkali metals). Thus, poorer agreement between calculations and experiment should be expected. According to figure 5 this is also the case. However, the Born-Haber cycle calculations performs well on a qualitative scale i.e. it predicts the correct order in thermodynamic stability: Ca being the most stable, Mg the least stable and Sr and Ba having roughly the same stability. When moving to the transition metals and the rare earth metals the Born-Haber predictions seem to break down due to a higher degree of metallic bonding character. Nonetheless, it still seem to have some limited applicability to the early transition metals forming hydrides under strongly exothermic conditions.

3.2 The Miedema model

Miedema and co-workers have proposed a semi-empirical model known as the *Miedema model* for the formation enthalpy of transition metal alloys and metallic alloys between transition metals and non-transition metals. The basis of the model

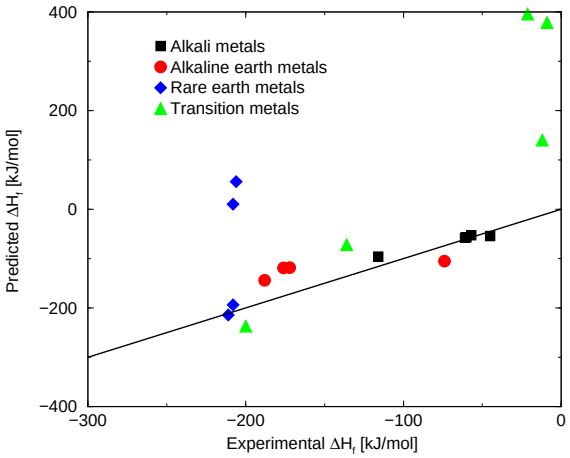

Figure 5. Predicted vs. experimental values for ΔH_f calculated from the Born-Haber cycle. Experimental determined ΔH_f for the alkali metal hydrides are from ref. [14], experimental ΔH_f for the alkaline rare earth metal hydrides are from ref. [15], experimental ΔH_f for the rare earth metal hydrides are from ref. [12] and experimental ΔH_f for the transition metals are from ref. [11, 15]. The full line represents the case when pred. equal exp.

is the Wigner-Seitz concept of atomic cells. For a detailed description of the model we refer to ref. [16, 17, 18, 19]. The Miedema model have also been extended to account for hydride formation enthalpies of binary metal hydrides [15, 19, 20].

The alloy formation can be described by the following reaction.

$$yA + zB \rightleftharpoons A_yB_z \tag{10}$$

With y and z being the stoichiometric coefficients of A and B, respectively. The enthalpy of formation of the alloy, $\Delta H_{A_yB_z}$ is given by:

$$\Delta H_{A_yB_z} = \Delta H'_{A_yB_z} + y\Delta H_A^{trans} + z\Delta H_B^{trans} \tag{11}$$

Assuming that A and B are metallic $\Delta H'_{A_yB_z}$ can be calculated by the Miedema formalism

$$\Delta H'_{A_yB_z} = \frac{2f(c^s)(c_A V_A^{2/3} + c_B V_B^{2/3})}{(n_{ws}^A)^{-1/3} + (n_{ws}^B)^{-1/3}} \times \left[-P(\Delta\Phi^*)^2 + Q(\Delta n_{ws}^{1/3})^2 - R\right] \tag{12}$$

where c_A and c_B are atomic concentrations of elements A and B, V_A and V_B are the molar volumes, $\Delta\Phi^* = \Phi_A^* - \Phi_B^*$ is the difference in electronegativity, $\Delta n_{ws}^{1/3} = (n_{ws}^A)^{-1/3} - (n_{ws}^B)^{-1/3}$, where n_{ws}^A and n_{ws}^B are the electron densities of A and B at the boundary of their Wigner-Seitz cells, respectively, Q, P and R are constants, and $f(c^s)$ is a function of the atomic concentrations given by:

$$f(c^s) = c_A^s c_B^s \left[1 + 8(c_A^s c_B^s)^2\right] \tag{13}$$

with

$$c_A^s = \frac{c_A V_A^{2/3}}{c_A V_A^{2/3} + c_B V_B^{2/3}} \tag{14}$$

$$c_B^s = \frac{c_B V_B^{2/3}}{c_A V_A^{2/3} + c_B V_B^{2/3}} \tag{15}$$

The H^{trans} in eq. 11 is included to account for transformation from non-metallic to metallic state e.g. if A is a metal and B is hydrogen ΔH_A^{trans} is zero and ΔH_B^{trans}

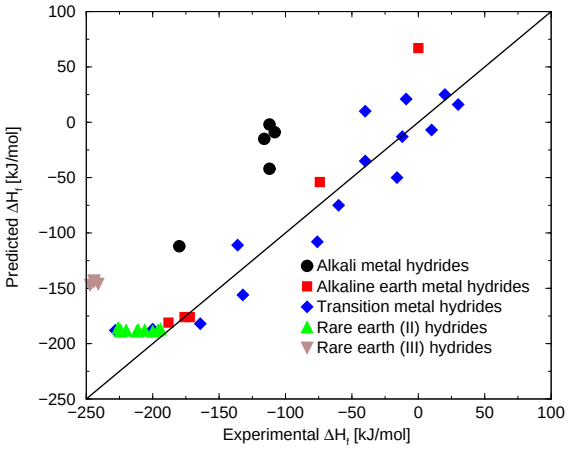

Figure 6. Predicted values of the formation enthalpy of binary metal hydrides obtained from Miedema model calculations vs. experimental values. Values are adapted from ref. [15].

is non-zero since hydrogen is non-metallic in its ground state. The energy required to transform gaseous hydrogen into metallic hydrogen have been estimated to approx. 100 kJ/mol H [19]. The Miedema model have also been extended to predict hydrogen content in binary hydrides of the form AH_z [15]. This is simply done by replacing y and z with 1/(1+x) and x/(1+x), respectively. The formation enthalpy can now be written as:

$$\Delta H'_{AH_x} = (1+x)\Delta H'_{A_{1/(1+x)}B_{x/(1+x)}} \tag{16}$$

The hydrogen content is now determined as the value of x giving the most stable configuration i.e. the minimum enthalpy.

The performance of the Miedema model is evaluated by comparing predicted values of the hydride formation enthalpies with experiments for a large number of binary hydrides. This is shown in figure 6.

From the figure it is obvious that the Miedema model generally performs well predicting the formation enthalpy of binary transition metal hydrides. This is consistent with the picture drawn in ref. [19]. The model also perform well predicting ΔH_f for divalent rare earth hydrides. However, the formation enthalpy of the trivalent rare earth hydrides seem to be under-predicted by approx. 100 kJ/mol. Surprisingly, the model also does a good job (except for Be) predicting the formation enthalpy of the alkaline earth metal hydrides. This could suggest that the bonding character in these compounds are in fact less ionic than suggested by the Born-Haber calculations in the previous section. The Miedema model generally under predicts the formation enthalpy of the alkali metal hydrides by approx. 75 kJ/mol H_2.

3.3 Advanced methods

In the previous sections we have had our focus on simple empirical models. While attractive due to the fact that they offer estimates of formation enthalpies with only little computational effort, the level of detail is limited. In this section we will turn our focus towards more advanced methods with emphasis on EMT (Effective Medium Theory) calculations and DFT (Density Functional Theory) calculations.

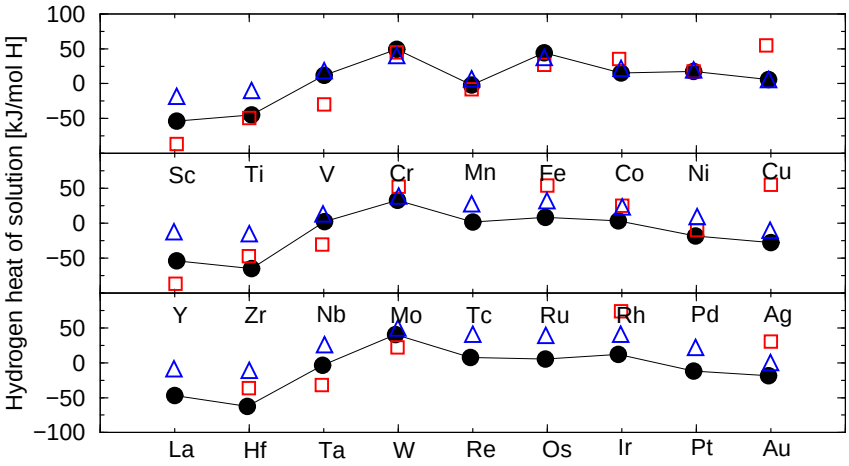

Figure 7. Heats of solution of hydrogen in transition metals. Filled circles are calculated values, Open squares are experimental values and open triangles the contribution to the heat of solution from ΔE^{eff}_{hom}. The interstitial positions hosting the hydrogen atom are chosen as tetrahedral in BCC metals and octahedral in FCC and HCP metals. All values are extracted from ref. [21, 22].

Effective Medium Theory

The Effective Medium Theory was originally developed by Nørskov and co-workers and applied to the calculation of binding energies of small atoms in metals. EMT offers a simplified way of calculating total energies in contrast to *ab initio* methods. In EMT the surroundings of an embedded atom (in this case hydrogen) is approximated by a homogeneous electron gas. The total energy for embedding a hydrogen atom in position $\boldsymbol{R}$ into a transition metal can be expressed by the following summation

$$\Delta E(\boldsymbol{R}) = \Delta E^{eff}_{hom}(\bar{n}_0(\boldsymbol{R})) + \Delta E_c(\boldsymbol{R}) + \Delta E_v(\boldsymbol{R}) + \Delta E^{hyb}(\boldsymbol{R}) \tag{17}$$

where $\Delta E^{eff}_{hom}(\bar{n}_0(\boldsymbol{R}))$ describes the interaction between the embedded hydrogen atom and the homogeneous electron gas with electron density $\bar{n}_0$. $\Delta E_c(\boldsymbol{R})$ is a correction term describing interaction between the metal cores and the hydrogen atom. $\Delta E_v(\boldsymbol{R})$ is a correction term dependent on the definition of $\Delta E^{hyb}(\boldsymbol{R})$. $\Delta E^{hyb}(\boldsymbol{R})$ is a hybridization term describing hybridization between hydrogen and the metal d electrons. For a more detailed description of the basis and applications of EMT we refer to ref. [21, 22, 23, 24] and references within.

When calculating $\Delta E(\boldsymbol{R})$ typically an appropriate unit cell of the host metal metal is chosen with finite size. The total electronic energy is then evaluated by inserting n H atoms in the metal host. The formation enthalpy is evaluated by

$$\Delta H_f = E^{tot}_{metal+H} - E^{tot}_{metal} - \frac{n}{2}E^{tot}_{H_2} \tag{18}$$

with $E^{tot}_{metal+H} = \Delta E(\boldsymbol{R})$. If n is small ($= 1$) the heat of solution is evaluated and if n is large (close to the stoichiometry of the hydride) the hydride formation enthalpy is evaluated.

Nørskov and co-workers [21, 22] have used EMT to calculate the heat of solution of hydrogen in 27 $3d$, $4d$ and $5d$ transition metals. The result is shown in figure 7. From the figure it is noticed that the EMT generally does a good job predicting the trend in heats of solution of hydrogen in transition metals. However, the early and late transition metals seem to be under and over predicted, respectively by the model. There are also other interesting properties: *i)* There is a tendency for

	Heat of solution [kJ/mol H]		Heat of formation [kJ/mol H]	
	Calc.	Exp.	Calc.	Exp.
Ni	29	27	11	5
Pd	-12	-16	-17	-20
Pt	25	38	8	—

Table 2. Heats of solution and heats of hydride formation of Ni, Pd and Pt determined by EMT-calculations and compared with experiments. All data are read graphically from ref. [23]. The calculated values have not been corrected with thermal or zero point energies. In the case of Pd the calculated energy should be reduced by approx. 7 kJ/mol by doing so [23].

stronger binding to the left in the periodic table *ii)* The variation in the heat of solution is more or less governed by changes in $\Delta E^{eff}_{hom}(\bar{n}_0(\boldsymbol{R}))$. $\Delta E^{eff}_{hom}(\bar{n}_0(\boldsymbol{R}))$ is roughly proportional to the electron density. *ii)* The heats of solution show a broad maximum near the middle of the transition metal series. This may be accounted for by the fact that the electron density shows a maximum around the middle of the transition metals where the *d*-band is half filled (this is reflected in a maximum in $\Delta E^{eff}_{hom}(\bar{n}_0(\boldsymbol{R}))$).

Christensen et al. [23] calculated both heats of solution of hydrogen in Ni, Pd and Pt and heats of formation of the corresponding hydrides. The results of their calculations are summarized in table 2 together with experimental determined values.

From table 2 it is observed that despite the crudeness of the calculations experimental values are successfully reproduced. More important is the fact that the model predicts the trend that H in Ni is endothermic (and probably also in Pt) while H in Pd is endothermic. The reason for this may be accounted for by considering the difference in interstitial electron density in the two metals. Ni has a smaller lattice constant (3.52 Å) compared to Pd (3.89 Å) and thereby a larger interstitial electron density. This is reflected in a higher heat of solution and a higher heat of formation, respectively, due to the $\Delta E^{eff}_{hom}(\bar{n}_0(\boldsymbol{R}))$ contribution in eq. 17. Based on total energy calculation at varying hydrogen content the authors propose that the fact the hydride phase is stable with hydrogen content above x = 0.6 is due to the level off in H-H attractions.

Density Functional Theory

The Hamiltonian, *H*, of a system with N electrons and M nuclei under the Born-Oppenheimer approximation is

$$H = \sum_i^N -\frac{1}{2}\nabla_i^2 + \sum_{i<j}^N \frac{1}{|\mathbf{r}_i - \mathbf{r}_j|} - \sum_{i,l}^{N,M} \frac{Z_l}{|\mathbf{r}_i - \mathbf{R}_l|} + \sum_{k<l}^M \frac{Z_l Z_k}{|\mathbf{R}_k - \mathbf{R}_l|} \tag{19}$$

where $\mathbf{r}$ and $\mathbf{R}$ are the coordinates of the electrons and nuclei, respectively. The first term is the kinetic energy operator for the electrons, the second term is the electron-electron repulsion, the third and fourth term are the electron-nucleus and nucleus-nucleus interactions, respectively.

Wave function methods such as Hartree-Fock (HF) and configuration interaction (CI) try to determine the N-electron eigenfunction to the *Schrödinger* equation corresponding to the Hamiltonian (Eq. 19) under the constraint of antisymmetry with respect to interchange of two electrons. Density Functional Theory (DFT) takes a fundamentally different approach. In DFT the fundamental variable is not

the wave function, but the corresponding observable electron density, n($\mathbf{r}$)

$$n(\mathbf{r}) = \sum_{\sigma} d\sigma \int d\mathbf{x}_2 \cdots \int d\mathbf{x}_N |\psi(\mathbf{r}\sigma, \mathbf{x}_2 \ldots, \mathbf{x}_N)|^2, \tag{20}$$

where the integrals over $\mathbf{x}_i$ denote sums over the spin coordinates σ_i and integrals over the space coordinates $\mathbf{r}_i$. Hohenberg and Kohn [25] proved that the total energy of a system of interacting electrons is a unique functional of the electron density. It was further proven that the ground state density minimizes the functional (variational principle). Hence it is possible to obtain the ground state total energy of the system by minimizing the total energy, E[n($\mathbf{r}$)], with respect to the electron density under the constraint that the particle number is conserved. The theorems imply that the original 3N dimensional problem of finding the N-electron wave functions can in principle be reduced to a 3 dimensional problem of finding the density.

Kohn and Sham [26] wrote the energy functional as

$$E[n] = T_0[n] + \int d\mathbf{r} n(\mathbf{r}) V_{ex}(\mathbf{r}) + \frac{1}{2} \int d\mathbf{r} n(\mathbf{r}) \int d\mathbf{r}' \frac{n(\mathbf{r}')}{|\mathbf{r} - \mathbf{r}'|} + E_{xc}[n], \tag{21}$$

where $T_0[n]$ is the exact kinetic energy of N non-interacting electrons with the density n. E_{xc} is termed the exchange-correlation energy, and is the only term not known exactly.

Solving the Kohn-Sham equations [26]

$$\left(-\frac{1}{2}\nabla^2 + \nu \right) \psi_i(\mathbf{r}) = \epsilon_i \psi_i(\mathbf{r}) \tag{22}$$

with the constraint

$$\sum_{i=1}^{N} |\psi_i(\mathbf{r})|^2 = n(\mathbf{r}) \tag{23}$$

the kinetic energy of the non-interacting electron gas, $T_0[n(\mathbf{r})]$, is obtained as

$$T_0[n(\mathbf{r})] = \sum_{i=1}^{N} \epsilon_i + \int \nu(\mathbf{r}) n(\mathbf{r}) d\mathbf{r} \tag{24}$$

ν is the effective one-electron potential and the ground state is given by

$$\nu(\mathbf{r}) = \phi(\mathbf{r}) + \nu_{xc}(\mathbf{r}) \tag{25}$$

where $\phi(\mathbf{r})$ is the electrostatic potential

$$\phi(\mathbf{r}) = \nu_{ex}(\mathbf{r}) + \int \frac{n(\mathbf{r}')}{|\mathbf{r} - \mathbf{r}'|} d\mathbf{r}' \tag{26}$$

and the exchange and correlation potential is defined as

$$\nu_{xc}(\mathbf{r}) \equiv \frac{\delta E_{xc}[n(\mathbf{r})]}{\delta n(\mathbf{r})}. \tag{27}$$

By solving Eq. 22 and 22 self-consistently the ground state energy E_0 and density n_0 can be obtained. The problem has been reduced to solving a system of N non-interacting electrons. The above procedure is in principle exact, but approximations will enter because $E_{xc}[n(\mathbf{r})]$ is not known explicitly. $E_{xc}[n(\mathbf{r})]$ contains the many-body complications. For additional details about exchange-correlations, $\mathbf{k}$-point sampling, cut-off energy etc. we refer to ref. [26, 27, 28, 29, 30, 31].

The literature contains many examples of the application of DFT to binary metal hydrides. However, in brief we will only use a few representative examples.

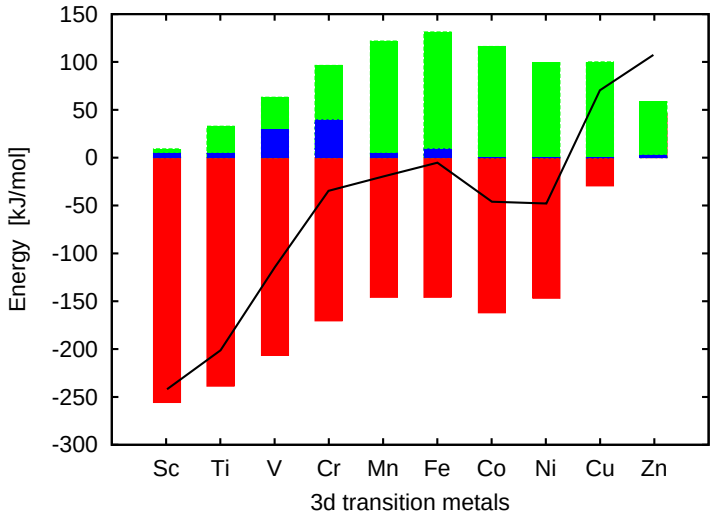

*Figure 8. Trend in formation enthalpy for 3*d *transition metal dihydrides with the CaF_2 structure (full line). The red bars represent $E_{hydride}$, blue bars represent $E_{transform}$ and green bars represent $E_{expansion}$. All data points are adapted from ref. [34].*

Yu and Lam have studied the electronic and structural properties of MgH_2 using DFT [32]. Assuming the experimentally stable rutile structure of MgH_2 they minimized the total energy by optimizing the lattice parameters. The calculated equilibrium values agreed to within 2.2 % of the experimentally determined values. Analysis of the electronic properties show that MgH_2 is an insulator with a band gap of 3.06 eV. However, this is 2 eV lower than the experimentally determined band gap. The cohesive energy is found to be 11.2-13.5 eV (exp. 13.56 eV). From this the enthalpy of formation of magnesium hydride is approximated to be between $\Delta H_f = -38.4$ kJ/mol H_2 to $\Delta H_f = -72$ kJ/mol H_2 (exp. $\Delta H_f \approx -75$ kJ/mol H_2). The discrepancy between theory and experiment may probably be assigned to the choice of the LDA (Local Density Approximation) exchange-correlation.

Both Miwa and Fukumoto [33] and Smithson et al. [34] made first principles study of the interaction of hydrogen with transition metals within the DFT formalism. While Miwa and Fukumotos investigation is restricted to Ti, V, Cr, Fe and Ni Smithson et al. have calculated formation energies for all $3d$ and $4d$ transition metal hydrides. Despite the use of different exchange-correlations (Miwa and Fukumoto use GGA while Smithson et al. use LDA) the authors reach quite similar conclusions. It is generally found that the early transition metals form stable hydrides and that the formation enthalpy is rapidly lowered when moving to the right in the transition metals. Around the middle this trend levels off and a slight increase in the formation energy is found when moving further to the right [33, 34]. To the far right (noble metals) a huge increase in the formation energy is found implying that these hydrides are unstable [34]. This is all illustrated for dihydrides with the CaF_2 structure by the full line in figure 8. Furthermore, ΔH_f may be decomposed into the following three parts [33, 34]

$$\Delta H_f = E_{transform} + E_{expansion} + E_{hydride} \tag{28}$$

where $E_{transform}$ is the energy required in order to transform the host metal lattice into the arrangement of the metal ions in the metal hydride, $E_{expansion}$ is the energy required to expand the host metal lattice to that of the hydride and finally $E_{hydride}$ is the hydrogen insertion energy in the expanded metal lattice. All

Compound	Structure	ΔH_f(DFT) [kJ/mol H]	ΔH_f(Exp) [kJ/mol H]	Ref.
LiH	NaCl	-87	-116	[14]
NaH	NaCl	-43	-56.5	[14]
KH	NaCl	-41	-57.7	[14]
MgH_2	TiO_2	-32	-37	[15]
CaH_2	Co_2Si	-86	-94	[15]
SrH_2	Co_2Si	-84	-88	[15]
BaH_2	Co_2Si	-72	-86	[15]
ScH_2	CaF_2	-100	-100.5	[35]
TiH_2	CaF_2	-76	-68	[15]
V_2H	β_1-V_2H	-42	-40.6	[35]
VH_2	CaF_2	-33	-16	[11]
NiH_x	NaCl	-7.5	-4.5	[15]
YH_3	BiF_3	-79	-79.8	[35]
YH_2	CaF_2	-105	-114	[15]
PdH_x	NaCl	-18	-20	[15]
LaH_2	CaF_2	-95	-104	[12]
LaH_3	BiF_3	-78	-82.5	[15]

Table 3. Formation enthalpies for binary metal hydrides from DFT-calculations and experiments. All calculated values are from ref. [35].

three contributions are also mapped in figure 8.

From figure 8 we note that the lattice expansion energy $E_{expansion}$ increases from the left until Fe and subsequently decreases. This may be explained from the cohesion energy which have its maximum around the middle of the transition metals where the d-band is half filled and decreases when the d-band filling is higher and lower, respectively. The structural transformation energy $E_{transform}$ is low when host metal structure is close to that of the hydride. This is the case for more or less most of the metals except for V and Cr which have stable bcc structures. The remaining contribution to ΔH_f is $E_{hydride}$ and this is by far the most important contribution. We note that the trend in $E_{hydride}$ is directly reflected in the trend for ΔH_f. Miwa and Fukumoto [33] suggested a simple relation between the hydrogen insertion energy and the interstitial hole size in the metal lattice of the following form

$$E_{hydride} = \alpha R^{-n} - \beta \tag{29}$$

where α, n and β are fitting parameters and R is the hydrogen-metal interatomic distance. The above relation implies that the larger the interstitial hole size the more energetically favorable is the hydrogen insertion.

Smithson et al. also performed total energy DFT-LDA calculation for the hydrides of the alkali metals and the alkaline earth metals [34]. In the case of the alkali metal hydrides all adopt the NaCl structure and calculations qualitatively predicted the trend in hydride stability. However, the calculations generally seemed to over predict the stability. For the alkaline earth metals the correct structure of the hydrides are predicted (rutile for MgH_2 and Co_2Si for Ca, Sr, Ba). However, quantitatively the enthalpy of formation is only within 50 kJ/mol of experimentally observed values.

To test the performance in general of DFT as a method of predicted ΔH_f we use the results of Wolverton et al. [35] who performed calculations of a number of selected alkali, alkaline earth and transition metal hydrides using DFT-GGA. We believe that GGA exchange-correlation generally performs better than LDA. Further, the description of gas phase H_2 and vibrational entropy contributions

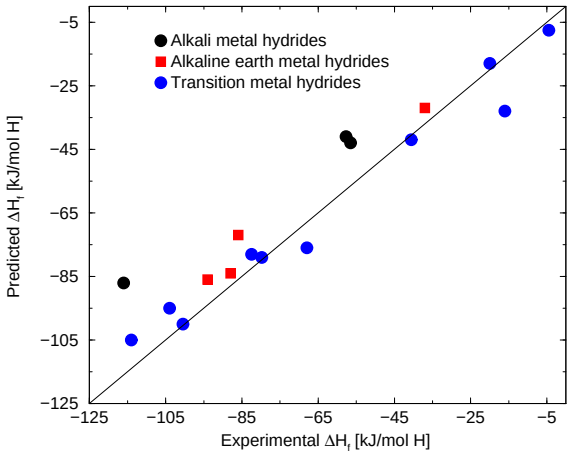

Figure 9. Predicted values of the formation enthalpy of binary metal hydrides obtained from DFT-GGA calculations [35] vs. experimental values from ref. [14, 11, 12, 15].

from the solid state phases by Wolverton et al. seems more realistic than that of Smithson et al.

The results of the calculations of Wolverton et al. are summarized in table 3 along with experimental values. As also shown in the table the structure of the hydride is also given and the selected metal hydrides cover not only many different kinds of metals but also many different kinds of structures with different kinds of environments for inserted hydrogen atoms. The agreement between calculations and experiment is also summarized in figure 9. The agreement between calculations and experiment is generally quite good. The DFT-GGA calculations are superior to Born-Haber cycle calculations cf. figure 5 and also better than the Miedema model cf. figure 6. Direct comparison with the EMT calculations cf. 7 is difficult since only transition metals are dealt with using this method. However, on a more specific basis the DFT-GGA calculations seem to under predict the stability of the alkali metal hydrides but not as bad as the Miedema model. Besides this discrepancy it performs excellent predicting ΔH_f for both alkaline earth metal hydrides and transition metal hydrides including the di- and tri hydride of La.

4 Ternary hydrides

Until now we have had our focus on the binary metal hydrides and experimental results of the enthalpy of hydride formation show that these cover a wide range in stability going from the highly stable hydrides ($\Delta H_f << 0$) of the alkali metals, alkaline earth metals, rare earth metals and early transition metals to the much less stable hydrides of the metal hydrides around the middle of the transition metals ($\Delta H_f < 0$) towards the unstable hydrides of the late transition metals ($\Delta H_f > 0$). As mentioned previously the criterion for the formation enthalpy was $\Delta H_f > -48$ kJ/mol H_2. This should easily be met by a proper choice of binary metal hydride. However, if the energy density criterion should also be met the task may not seem that easy. In figure 10 the gravimetric hydrogen density $\rho_{H_2}(m)$ is plotted as a function of ΔH_f for most the binary metal hydrides investigated so far. From the figure it is obvious that none of the metal hydrides fulfill both the hydrogen density criterion and the thermodynamic stability criterion. This is of course old news and as a natural consequence the search for better hydrogen storage materials continue among the ternary metal hydrides.

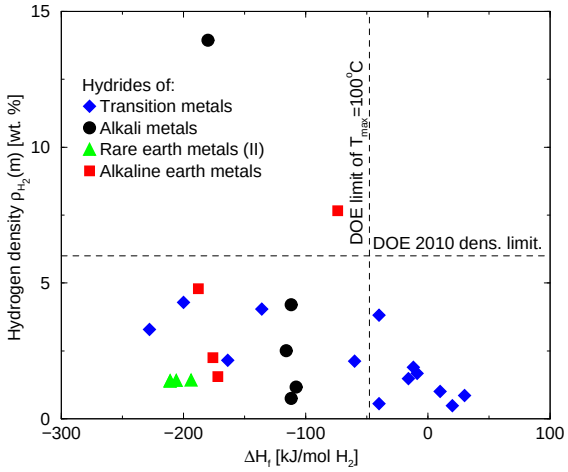

Figure 10. Relationship between the gravimetric hydrogen density and the experimentally observed formation enthalpy [15] of selected binary hydrides of alkali metals, alkaline earth metals, transition metals and rare earth metals.

4.1 A simple model

In order to develop a simple empirical model for ΔH_f of ternary hydrides we shall examine the effect of *alloying*[2] two binary metal hydrides. In figure 11 A-D ΔH_f for $LaNi_5H_6$, Mg_2NiH_4, $TiFeH_2$, and Mg_2FeH_6 are shown along with ΔH_f for their binary hydride constituents. Each plot is organized in the following manner: placed to left is the metal forming the most stable hydride e.g. for $LaNi_5$ it is La, in middle we have the ternary hydride and placed to the right is the metal forming the least stable hydride e.g. for $LaNi_5$ this is Ni.

According to figure 11 A-C ΔH_f of the ternary hydride is somewhere in between that of the two binary hydride constituents[3]. This is in fact also the case for many

[2]This term is purely used for illustrational reasons. In practice the ternary hydride is often formed by first alloying the metal constituents and then subsequently hydriding the metal alloy into a ternary hydride.

[3]Whenever Fe appears the bar representing ΔH_f seems to be missing. This is not an error,

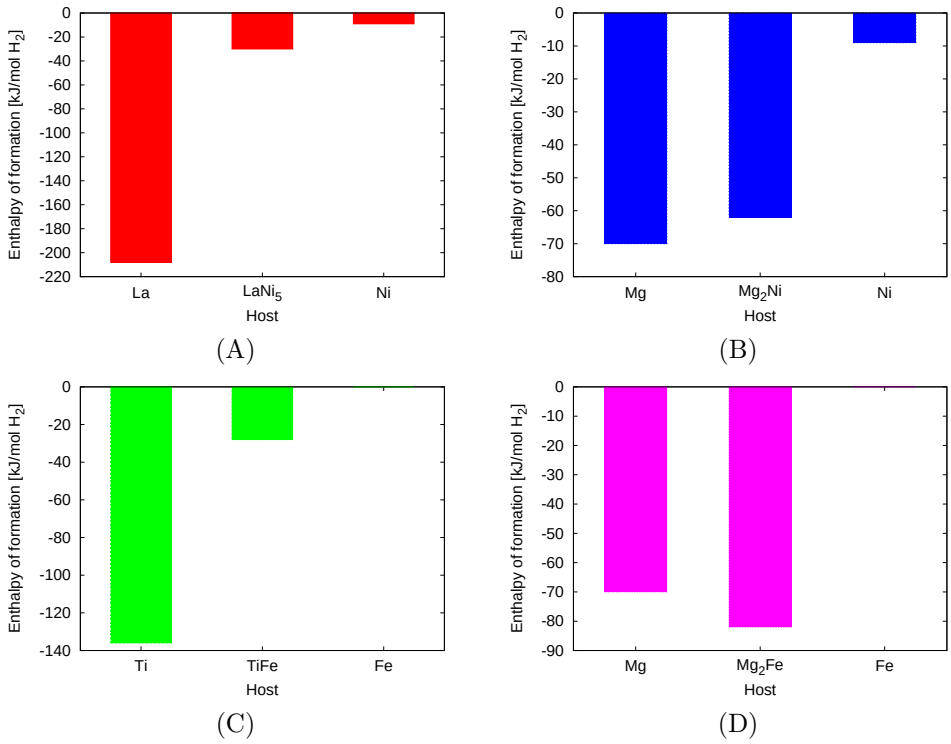

Figure 11. Enthalpy of formation of ternary hydrides and compared to their corresponding binary hydrides. A: LaH_2, $LaNi_5H_6$ and NiH [12, 5, 15], B: MgH_2, Mg_2NiH_4 and NiH [15, 36, 37], C: TiH_2, $FeTiH_2$ and FeH [38, 5, 15], D: MgH_2, Mg_2FeH_6 and FeH [15, 36, 37]

other ternary hydrides e.g. $ZrCr_{1.8}$, $TiCr_{1.8}$, $ZrMn_2$, ZrNi, $CaNi_5$, $NaAlH_5$, $LiBH_4$ (cf. figure 3, table 5 and ref. [5, 15, 12]). From the figure we note that the effect of alloying with Ni has the largest effect (more pronounced lowering ΔH_f) of $LaNi_5$ compared to Mg_2Ni. This suggests that ΔH_f of the ternary hydride is related to stoichiometry of the two host metals. Thus increasing the amount of weakly hydride forming metal reduces ΔH_f of the alloy. We propose the following model for ΔH_f of a ternary metal hydride AB_xHy as a weighted average of ΔH_f for the binary metal hydrides

$$\Delta H_f(A_xB_yH_{u+v}) = \frac{x}{x+y}\Delta H_f(AH_u) + \frac{y}{x+y}\Delta H_f(BH_v) \tag{30}$$

based on the following general reaction equation describing *alloying* of two binary metal hydrides

$$xAH_u + yBH_v \rightleftharpoons A_xB_yH_{u+v} \tag{31}$$

By convention A refers to the metal forming a the most stable hydride and B refers to the weakly hydride forming metal (compared to A).

Equation 30 explicitly states that ΔH_f of the ternary hydride can be modified by either changing $\Delta H_f(AH_u)$ or $\Delta H_f(BH_v)$ by substitution e.g. the less stable BH_v is the less stable will the ternary hydride be. However, according to figure 11 B and D when substituting Ni with Fe in Mg-alloys the opposite is observed experimentally clearly indicating a limitation in the model. Further, experimental observations suggests that replacing La in $LaNi_5$ with another rare earth metal e.g. Pr or Ce the stability of the ternary hydride decrease in the following order $LaNi_5$

but due to the fact that ΔH_f for iron hydride is close to zero or even slightly positive.

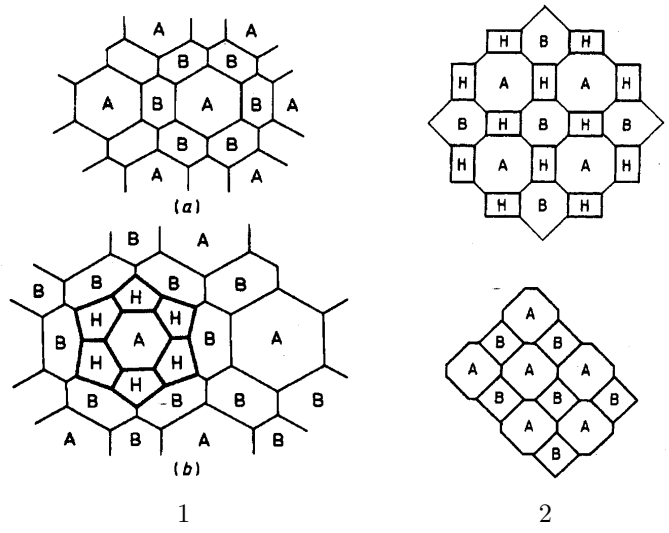

Figure 12. Schematic of the hydrogen positions in AB_n alloys. To the top left is shown an alloy poor in component A (hydride forming). Below is the corresponding hydride. To the lower right an AB (n=1) type alloy rich in A is shown with its corresponding allow (above). Adapted from ref. [19, 39].

$>$ $PrNi_2$ $>$ $CeNi_5$ [5]. However, ΔH_f of the rare earth metal hydrides increase in the following manner LaH_2 $<$ PrH_2 $<$ CeH_2 [15]. Thus, according to eq. 30 the opposite trend in ΔH_f of $ReNi_5$ is predicted. Again the model shows clear limitations. Henceforth a better suited model is called upon.

4.2 The rule of reversed stability

Miedema and coworkers have proposed a model to predict ΔH_f for ternary hydrides [19, 39]. This model is also known as the rule of reversed stability (which become clear in moment) and ΔH_f of the ternary hydride (AB_nH_{x+y}) is given by

$$\Delta H_f = \Delta H(AH_x) + \Delta H(B_nH_y) - \Delta H(AB_n) \tag{32}$$

where A is a transition metal forming a stable hydride e.g. Sc, Y, La, Ti, Zr, Hf, Th, U, and Pu, B is an arbitrary transition metal, $\Delta H(AH_x)$ is the heat of formation of the hydride of A, $\Delta H(B_nH_y)$ is the heat of formation of the hydride of B, and $\Delta H(AB_n)$ is the heat of formation of the AB_n alloy. According to eq. 32 the more stable an alloy A and B forms the less stable will the corresponding hydride be, hence the name of the model. This feature is the only difference between this model and the simple model proposed in the previous section i.e. ΔH_f is also proportional to the heat of formation of the binary hydrides of A and B.

The input to the model is either experimentally known heats of formation of the binary hydrides of A and B and heat of formation of the AB_n alloy or estimated values using the Miedema model described previously. The basis of the model is the assumption that the bonds/contacts between neighboring A and B atoms are at least partially broken upon hydrogenation due to hydrogen surrounding A atoms. This is shown in figure 12.1.

Relation 32 only holds for compounds with large n corresponding to figure 12.1 where all contacts between A and B atoms are broken due to insertion of hydrogen e.g. $LaNi_5$. In order to have more general applicability viz. for smaller values of n

Metal A	AB_n	AB_nH	x	y	F
Ti, Hf, Zr,	AB_5	AB_5H_5	2	3	0.1
V, Nb, Ta, Sc	AB_3	AB_3H_4	2	2	0.2
	AB_2	$AB_2H_{3.5}$	2	2.5	0.4
	AB	ABH_2	1.5	0.5	0.6
La, Y, Re,	AB_5	AB_5H_6	2.5	3.5	0.1
Th, U, Pu	AB_3	AB_3H_5	2.5	2.5	0.2
	AB_2	AB_2H_4	2.5	1.5	0.4
	AB	$ABH_{2.5}$	2	0.5	0.6

Table 4. Formation enthalpies for binary metal hydrides from DFT-calculations and experiments. All calculated values are from ref. [35].

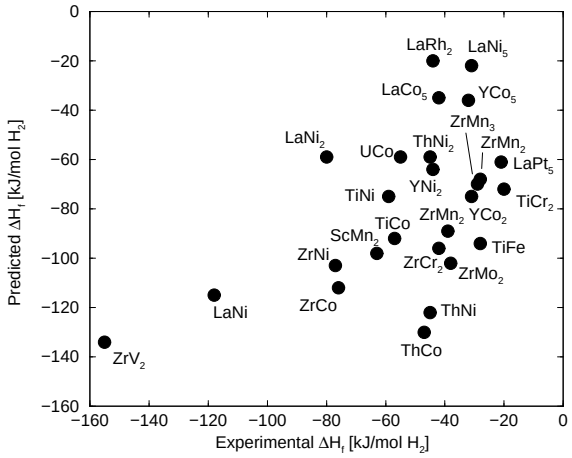

Figure 13. Predicted values of the formation enthalpy of intermetallic ternary hydrides obtained from Miedema model calculations [19] and the rule of reversed stability vs. experimental values [5, 15].

(but still $n \geq 1$) 32 is modified to

$$\Delta H_f = \Delta H(AH_x) + \Delta H(B_nH_y) - (1-F)\Delta H(AB_n) \tag{33}$$

where F varies with alloy composition, n,: the more rich in B (small n) the larger value of F in order to compensate for the fact that not all bonds between A and B atoms are broken upon hydrogenation if n is small cf. figure 12.2. Miedema and coworkers have proposed the values of F shown in table 4 along with values of n and m.

In order to validate we model we inspect model predictions versus experimentally determined values of ΔH_f. The model predictions are based on the rule of reversed stability with enthalpy of formation of both A and B hydrides and the AB alloy calculated from the Miedema model [19]. This is shown in figure 13 where the data of the hydrides of 9 AB, 12 AB_2, 1 AB_3, and AB_5 compounds are plotted. From the figure we note that the data points of ΔH_f seem to be more scattered for the ternary hydrides than for the binary hydrides using the Miedema model. This suggest that the increased scatter is introduced by the rule of reversed stability. With the rule of reversed stability initially being derived for large values of n it is perhaps not that surprising to see that the model does a reasonable job with the AB_5 hydrides (with exception of $LaPt_5$[4]). The rule of reversed stabil-

[4]The estimated value of ΔH_f for $LaPt_5$ was based on only one reported plateau pressure [5] and assuming ΔS = -130 J/(mol K). Thus even moderate experimental inaccuracies may effect

ity seems to generally over predict the value of ΔH_f hence predicting too stable ternary hydrides. Besides this trend the deviations from experiments seem to be rather unsystematic.

4.3 DFT

Unfortunately the literature on DFT applied to intermetallic hydrides is sparse. Due to this fact we will focus on two distinct group of hydrides: the magnesium based hydrides (hydrides of magnesium alloys) and the complex hydrides (alanates and borohydrides e.g. $NaAlH_4$ and $LiBH_4$).

Magnesium based hydrides

For simplicity we will in the following focus on the hydrogenation behavior of the Mg $3d$ transition metal alloys.

Magnesium is known to form an Mg_2Cu [40] alloy which disproportionates to magnesium hydride and $MgCu_2$ upon hydrogenation [41, 42].

$$2Mg_2Cu + 3H_2 \rightleftharpoons 3MgH_2 + MgCu_2 \tag{34}$$

From experiments ΔH_f have been reported to be approx. -70 kJ/mol H_2 (5 kJ/mol lower than for pure Mg).

Magnesium is also known to form a stable Mg_2Ni alloy [40] which forms a complex Mg_2NiH_2 hydride [5].

$$Mg_2Ni + 2H_2 \rightleftharpoons Mg_2NiH_4 \tag{35}$$

ΔH_f is approx. -62 kJ/mol H_2 [36, 5].

Magnesium does not form an alloy with Co. However applying ball milling sintering under hydrogen atmosphere produces a complex hydride [43] with ΔH_f of approx. 76 kJ/mol H_2 [36].

$$2Mg + Co + \frac{5}{2}H_2 \rightleftharpoons Mg_2CoH_5 \tag{36}$$

A compound more rich in magnesium (Mg_6CoH_{11}) have also been reported with $\Delta H_f = -89$ kJ/mol H_2

Magnesium does not form a stable Mg-Fe alloy either (calculations using the Miedema model shows a positive formation enthalpy for the formation of both Mg-Co and Mg-Fe [15]). Applying ball milling under hydrogen atmosphere produces a complex hydride [43] ΔH_f is approx. -77 kJ/mol H_2 [36]

$$2Mg + Fe + 3H_2 \rightleftharpoons Mg_2FeH_6 \tag{37}$$

Magnesium and manganese have shown to form a complex hydride. However, only if applying very high pressure of hydrogen ($\approx$ 20 kbar) and high temperature ($\approx$ 700 °C) [44]

$$3Mg + Mn + \frac{7}{2}H_2 \rightleftharpoons Mg_3MnH_7 \tag{38}$$

The compound decomposes around 280 °C. Assuming $\Delta S = -130$ J/(mol K) ΔH_f can be estimated to be approx. -72 kJ/mol H_2.

Vegge et al. [45] have investigated the trends in hydride formation of the MgTM alloys where TM is $3d$-transition metal belonging to the group Sc, Ti, V, Cr, Mn, Fe, Co, Ni, Cu, and Zn using DFT calculations. The authors use a body centered tetragonal unit cell for the MgTM structure with TM in the body center which is

the value of ΔH_f significantly.

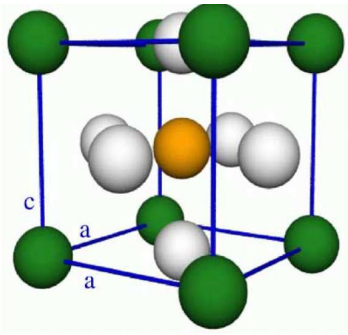

Figure 14. A schematic representation of the $MgFeH_3$ hydride in the Perovskite structure. Magnesium atoms at the corners (green), an iron atom in the center (orange), and hydrogen atoms at face centers (white). Figure is adapted from ref. [45].

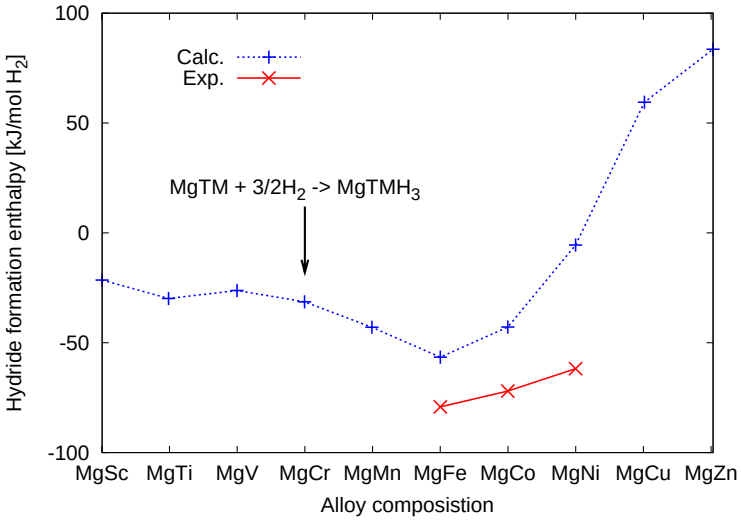

Figure 15. Trend in ΔH_f of the MgTM alloys. Calculated values are from [45] and experimental values of Fe, Co, and Ni are from [36]. Mn is estimated from [44].

initially relaxed. Sc, Co, Ni, and Cu relaxes in a bcc structure whereas the others remain tetragonal. For the hydrides a Perovskite structure is applied cf. figure 14 with the stoichiometry $MgTMH_3$ which remains cubic even after relaxation. The formation of hydride proceeds through the following reaction

$$MgTM + \frac{3}{2}H_2 \rightleftharpoons MgTMH_2 \tag{39}$$

For each of the MgTM hydrides the formation enthalpy is evaluated and the result is depicted in figure 15. The following trend in ΔH_f is observed: a gradual increase in the stability of the hydrides is observed going from MgSc to MgFe, which is followed by a rapid decrease in stability, resulting in $MgNiH_3$ hydride being only marginally stable and $MgCuH_3$ and $MgZnH_3$ unstable. The results are compared with literature data for ΔH_f of known MgTM hydrides as reviewed above. The experimental trend is the following: Mg_2Fe hydride is most stable thus stability decreases going both left to Mn and right towards Co and Ni. Mg_2Ni hydride is the least stable hydride. Despite the fact that the calculated values are

based on a different stoichiometry of both the MgTM alloys and the corresponding hydrides, respectively, compared to experimental observation (and thus different structure) the trend found using DFT resembles that of experiments. Although some shift in ΔH_f is observed probably due to differences in structure and stoichiometry. The fact that MgCu hydride is found unstable is also in agreement with experiments [41, 42]. Clearly DFT calculations are very useful in predicting trends in formation enthalpy of ternary metal hydrides.

Complex hydrides

The complex hydrides in particular the alanates and borohydrides with the general formula ABH_4, where A represents a metal (often an alkaline or an alkaline earth metal) and B represents either aluminum or boron, is perhaps some of the most promising materials for hydrogen storage.

For sodium aluminum hydride the decomposition is a multi step mechanism

$$(i) \quad : \quad NaAlH_4 \rightleftharpoons \frac{1}{3}Na_3AlH_6 + \frac{2}{3}Al + H_2 \tag{40}$$

$$(ii) \quad : \quad \frac{1}{3}Na_3AlH_6 \rightleftharpoons NaH + \frac{1}{3}Al + \frac{1}{2}H_2 \tag{41}$$

$$(iii) \quad : \quad NaH \rightleftharpoons Na + \frac{1}{2}H_2 \tag{42}$$

$$(i+ii) \quad : \quad NaAlH_4 \rightleftharpoons NaH + Al + \frac{3}{2}H_2 \tag{43}$$

$$(i+ii+iii) \quad : \quad NaAlH_4 \rightleftharpoons Na + Al + 2H_2 \tag{44}$$

Until recently this process was regarded as irreversible. However, in 1997 Bogdanović and Schwickardi showed that adding a Ti-compound catalyzed the reaction and thereby making it reversible [47]. The maximum hydrogen capacity of $NaAlH_4$ is 7.5 wt. %. However, this requires dehydrogenation of NaH which is very stable (decomposes around 425 °C [11]). Thus high temperature must be applied in order to achieve full dehydrogenation. For practical applications $NaAlH_4$ should only be dehydrogenated to Na_3AlH_6 (reaction $i+ii$) releasing 3.7 wt. % and 1.9 wt. % hydrogen respectivly resulting in a theoretical reversible capacity of 5.6 wt. % hydrogen. In practice a lower reversible capacity should be expected. The plateau pressure of reactions i and ii have been reported to be 1 bar at approx. 33 °C and 110 °C, respectively [46] cf. figure 16. NaAlH4 is very close in fulfilling the criterions formulated by the USDOE. This is the reason for the extensive reasearch effort devoted to complex hydrides and in particular $NaAlH_4$ including DFT calculations on the heat of formation of the hydrides.

Calculated heats of formation is indeed advantageous since the acquisition of thermodynamic parameters from experiment (PCI/Van't Hoff plot) is extremely tedious for the complex hydrides due to slow kinetics and limited reversibility. In table 5 calculated (DFT) heats of formation of the alkali alanates and alkali borohydrides, respectively, are compared with experimentally determined values either from calorimetric measurements or from PCI data. The values in table 5 are heats of formation of the hydrides from the elements in their standard states viz.

$$Na(s) + Al(s) + 2H_2(g) \rightleftharpoons NaAlH_4(s) \tag{45}$$

and

$$3Na(s) + Al(s) + 3H_2(g) \rightleftharpoons Na_3AlH_6(s) \tag{46}$$

In the literature a heat of reaction is often reported instead e.g. for reaction i and/or reaction ii. In order to back calculate the heat of formation of the hydrides

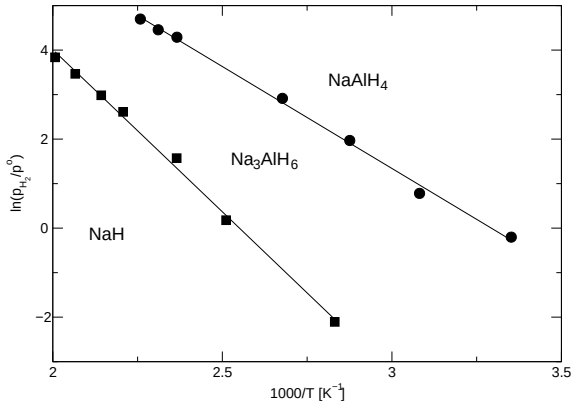

Figure 16. Van't Hoff plot for $NaAlH_4$. The stable hydride for each region of temperatures and pressures is marked on the graphic. Data points are taken from ref. [46].

as outlined above tabulated values of ΔH_f of the alkaline metal hydrides have been used [11].

From table 5 we note that there is generally excellent agreement between measured and calculated values of the alanates viz. $MAlH_4$. Unfortunately experimental information about the stability of M_3AlH_6 is sparse. However, for Na_3AlH_6 the agreement between experiment and theory is fairly good. The general agreement between experiment and calculation gives reason to believe that the calculated heats of formation of Li_3AlH_6 and K_3AlH_6 are indeed qualified estimates. For the borohydrides only experimentally determined values are available for the MBH_4 and not for M_3AlH_6 compounds. For MBH_4 calculations seem to agree with experiments. According to table 5 the reaction enthalpy of decomposition of $MAlH_4$ (reaction $i + ii$, $\Delta H(MAlH_4) - \Delta H(MH)$) and thus the decomposition temperature increase in the following sequence Li < Na < K. This is in agreement with experimentally observed decomposition temperatures [14, 48]. This is also the case for the borohydrides [11]. The most striking difference between the alanates and the borohydrides is the fact that the borohydrides are much more stable than the corresponding alanates [11, 14, 48]. This is also captured by the heats of formation obtained using DFT calculations.

It is interesting to note that none of the M_3BH_6 compounds are stable compared to their alkali metal metal hydride counterparts i.e. LiH, NaH and KH. This suggests that the decomposition of the borohydrides is likely different from the scheme outlined by reactions $i - iii$ [49, 50].

Alanates			
	Experimental	Theory	Ref.
$LiAlH_4$	-119	-113-(-107)	[51, 52, 53, 49]
$NaAlH_4$	-115-(-109)	-116-(-113)	[51, 54, 46]
$KAlH_4$	-166	-151-(-150)	[51, 53, 49]
Li_3AlH_6	—	-311-(-305)	[52, 53, 49]
Na_3AlH_6	-229-(-216)	-246-(-240)	[54, 46, 35, 53, 49]
K_3AlH_6	—	-276	[49]
Borohydrides			
	Experimental	Theory	Ref.
$LiBH_4$	-194	-180	[51, 49]
$NaBH_4$	-191	-198	[51, 49]
KBH_4	-229	-216	[51, 49]
Li_3BH_6	—	-54	[51, 49]
Na_3BH_6	—	45	[51, 49]
K_3BH_6	—	14	[51, 49]

Table 5. Comparison between formation enthalpies of alkali alanates and borohydrides from experiments and DFT calculations, respectively. Units are kJ/mol compound.

5 Summary

In this report a number of different ways of estimating the hydride formation enthalpy, ΔH_f, of both binary and ternary hydrides have been reviewed: Born-Haber cycle, The Miedema model, Effective Medium Theory, The rule of reversed stability, and Density Functional Theory. Based on evaluation of model performance by comparison with experimental data (both for binary hydrides and ternary complex hydrides) the most versatile and accurate method is found to be Density Functional Theory.

References

[1] L. Schlapbach, A. Züttel, Hydrogen-storage materials for mobile applications, Nature 414 (2001) 353–358.

[2] A. Züttel, Materials for hydrogen storage, Materials Today 9 (2003) 24–33.

[3] A. Züttel, Hydrogen storage methods, Naturwissenschaften 91 (2004) 157–172.

[4] http://www.eere.energy.gov/hydrogenandfuelcells/hydrogen/storage.html, U. S. Department of Energy, Last checked april 2004.

[5] Hydride information center, http://hydpark.ca.sandia.gov, last checked april 2004.

[6] C. E. Lundin, F. E. Lynch, C. B. Magee, A correlation between the interstitial hole sizes in intermetallic compounds and the thermodynamic properties of the hydrides formed from those compounds, Joural of the Less-Common Metals 56 (1977) 19–37.

[7] R. Griessen, A. Driessen, Heat of formation and band structure of binary and ternary metal hydrides, Physical Review B 30(8) (1984) 4372–4381.

[8] J. Smith, H. Van Ness, M. Abbott, Introduction to Chemical Engineering Termodynamics, fifh Edition, McGraw-Hill, 1996.

[9] C. E. Lundin, F. E. Lynch, Solid state hydrogen storage materials for application to energy needs, Tech. Rep. AFOSR-TR-76-1124, University of Denver, Denver, USA (1975).

[10] B. Vigeholm, Chemical energy storage based on metal hydrides, Tech. Rep. Risø-M-2608, Risoe National Laboratory, DK-4000 Roskilde, Denmark, (In Danish) (1989).

[11] D. R. Lide (Ed.), Handbook of Chemistry and Physics, 78th Edition, CRC Press LLC, 1997.

[12] W. M. Mueller, J. P. Blackledge, G. G. Libowitz (Eds.), Metal Hydrides, Academic Press, Inc., 1968.

[13] S. Elliott, Physics and Chemistry of Solids, John Wiley & Sons Ltd., 1998.

[14] W. Grochala, P. P. Edwards, Thermal decomposition of the non-interstitial hydrides for the storage and production of hydrogen, Chemical Reviews 104 (2004) 1283–1315.

[15] J. F. Herbst, On extending Miedema's model to predict hydrogen content in binary and ternary hydrides, Journal of Alloys and Compounds 337 (2002) 99–107.

[16] A. R. Miedema, P. F. de Châtel, F. R. de Boer, Cohesion in alloys - fundamentals of a semi-emperical model, Physica 100B (1980) 1–28.

[17] F. R. de Boer, R. Boom, W. C. M. Mattens, A. R. Miedema, A. K. Niessen, Cohesion in metals - transition metal alloys, Vol. 1 of Cohesion and structure, Elsevier Science Publishers B.V., 1988.

[18] A. R. Miedema, The electronegativity parameter for transition metals: heat of formation and charge transfer in alloys, Journal of the Less-Common Metals 32 (1973) 117–136.

[19] K. H. J. Buschow, P. C. P. Bouten, A. R. Miedema, Hydrides formed from intermetallic compounds of two transition metals: a special class of ternary alloys, Rep. Prog. Phys. 45 (1982) 937–1039.

[20] P. Bouten, A. R. Miedema, On the heats of formation of the binary hydrides of transition metals, Journal of the Less-Common Metals 71 (1980) 147–160.

[21] P. Nordlander, J. K. Nørskov, F. Besenbacher, Trends in the hydrogen heats of solution and vacancy trapping energies in transition metals, J. Phys. F: Met. Phys. 16 (1986) 1161–1171.

[22] J. K. Nørskov, F. Besenbacher, Theory of hydrogen interaction with metals, Journal of the Less-Common Metals 130 (1987) 475–490.

[23] O. B. Christensen, P. Stoltze, K. W. Jacobsen, J. K. Nørskov, Effective-medium calculations for hydrogen in Ni, Pd and Pt, Physical Review B 41 (18) (1990) 12413–12423.

[24] P. Stoltze, Simulation methods in atomic-scale materials physics, 1st Edition, Polyteknisk Forlag, 1997.

[25] P. Hohenberg, W. Kohn, Inhomogeneous Electron Gas, Phys. Rev. 136(3B) (1964) B864–B871.

[26] W. Kohn, L. J. Sham, Self-Consistent Equations including Exchange and Correlation effects, Phys. Rev. 140(4A) (1965) A1133–A1138.

[27] J. P. Perdew, J. A. Chevary, S. H. Vosko, K. A. Jackson, M. R. Pederson, D. J. Singh, C. Fiolhais, Atoms, Molecules, Solids, and Surfaces: Applications of the Generalized Gradient Approximation for Exchange and Correlation, Phys. Rev. B. 46 (1992) 6671.

[28] J. P. Perdew, K. Burke, M. Ernzerhof, Generalized Gradient Approximation Made Simple, Phys. Rev. Lett. 77(18) (1996) 3865–3868.

[29] M. C. Payne, M. P. Teter, D. C. Allan, T. A. Arias, J. D. Joannopoulos, Iterative Minimization Techniques for ab initio Total-Energy Calculations: Molecular Dynamics and Conjugate Gradients, Rev. Modern. Phys. 64 (1992) 1045–1097.

[30] H. J. Monkhorst, J. D. Pack, Special Points for Brillouin-Zone Integrations, Phys. Rev. B 13 (1976) 3865.

[31] D. J. Chadi, M. L. Cohen, Special Points in the Brillouin Zone, Phys. Rev. B 8 (1973) 5747.

[32] R. Yu, P. K. Lam, Electronic and structural properties of MgH_2, Physical Review B 37 (1988) 8730–8737.

[33] K. Miwa, A. Fukumoto, First-principles study on $3d$ transition-metal dihydrides, Physical Review B 64 (2002) 155114–1.

[34] H. Smithson, C. A. Marianetti, D. Morgan, A. Van der Ven, A. Predith, G. Ceder, First-principles study of the stability and electronic structure of metal hydrides, Physical Review B 66 (2002) 144107–1.

[35] C. Wolwerton, V. Ozoliņš, M. Asta, Hydrogen in aluminum: First-principles calculations of structure and thermodynamics, Physical Review B 69 (2004) 144109–1.

[36] A. Reiser, B. Bogdanović, K. Schlichte, The application of Mg-based metal-hydrides as heat energy storage systems, International Journal of Hydrogen Energy 25 (2000) 425–430.

[37] A. Pedersen, J. Kjøller, B. Larsen, B. Vigeholm, Magnesium for hydrogen storage, International Journal of Hydrogen Energy 8 (3) (1983) 205–211.

[38] J. F. Herbst, On estimating the enthalpy of formation and hydrogen content of quaternary hydrides, Journal of Alloys and Compounds 368 (2004) 221–228.

[39] A. R. Miedema, K. H. J. Buschow, H. H. Van Mal, Which intermetallic compounds of the transition metals form stable hydrides?, Journal of the Less-Common Metals 32 (1973) 117–136.

[40] P. Villars (Ed.), Pearson's Handbook Desk Edition, Vol. 2, ASM International, 1997.

[41] A. Karty, J. Grunzweig-Genossar, P. Rudman, Hydriding and dehydriding kinetics of Mg in a Mg/Mg_2Cu eutectic alloy: Pressure sweep method, Journal of Applied Physics 50 (11) (1979) 7200–7209.

[42] A. Andreasen, T. R. Jensen, A. M. Molenbroek, A. S. Pedersen, A study on the dehydrogenation of mgh_2/mg_2cu and $mgh_2/mgcu_2$, In preparation .

[43] J. Huot, E. Hayakawa, H. Akiba, Preperation of the hydrides Mg_2FeH_6 and Mg_2CoH_5, Journal of Alloys and Compounds 248 (1997) 164–167.

[44] K. Yvon, High pressure synthesis of new hydrogen storage materials, Tech. Rep. IEA Agreement on the Production and Utilization of Hydrogen, Task 12: Metal Hydrides and Carbon for Hydrogen Storage, Final Task Report 2001, International Energy Agency (2001).

[45] T. Vegge, L. S. Hedegaard-Jensen, J. Bonde, T. R. Munter, J. K. Nørskov, Trends in hydride formation energies for magnesium-3d transtion metal alloys, Journal of Alloys and Compounds Accepted.

[46] K. J. Gross, G. J. Thomas, C. M. Jensen, Catalyzed alanates for hydrogen storage, Journal of Alloys and Compounds 330-332 (2002) 683–690.

[47] B. Bogdanović, M. Schwickardi, Ti-doped alkali metal aluminium hydrides as potential novel reversible hydrogen storage materials, Journal of Alloys and Compounds 253-254 (1997) 1–9.

[48] J. A. Dilts, E. C. Ashby, A study of the thermal decomposition of complex metal hydrides, Inorganic Chemistry 11(6) (1972) 1230–1236.

[49] M. E. Arroyo y de Dompablo, G. Ceder, First principles investigation of complex hydrides AMH_4 and A_3MH_6 (A=Li, Na, K, M= B, Al, Ga) as hydrogen storage systems, Journal of Alloys and Compounds 364 (2004) 6–12.

[50] A. Züttel, P. Wenger, S. Rentsch, P. Sudan, P. Mauron, C. Emmenegger, $LiBH_4$ a new hydrogen storage material, Journal of Power Sources 118 (2003) 1–7.

[51] M. B. Smith, G. E. Bass Jr., Heats and free energies of formation of the alkali aluminum hydrides and cesium hydride, Journal of Chemical Engineering Data 8(3) (1963) 342–346.

[52] O. M. Løvvik, S. M. Opalka, H. W. Brinks, B. C. Hauback, Crystal structure and thermodynamic stability of the lithium alanates $LiAlH_4$ and Li_3AlH_6, Physical Review B 69 (2004) 134117.

[53] S. C. Chung, H. Morioka, Thermochemistry and crystal structure of lithium, sodium and potassium alanates as determined by ab initio simulations, Journal of Alloys and Compounds 372 (2004) 92–96.

[54] B. Bogdanović, R. Brand, A. Marjanović, M. Schwichardi, J. Tölle, Metal-doped sodium aluminium hydrides as potential new hydrogen storage materials, Journal of Alloys and Compounds 302 (2000) 36–58.

Bibliographic Data Sheet **Risø–R–1484(EN)**

Title and author(s)

Predicting formation enthalpies of metal hydrides

Anders Andreasen

ISBN	ISSN
87–550–3382–2 (Internet)	0106–2840

Dept. or group	Date
Materials Research Department	October 2004

Groups own reg. number(s)	Project/contract No.

Sponsorship

Pages	Tables	Illustrations	References
33	5	16	54

Abstract (Max. 2000 char.)

In order for the *hydrogen based society* viz. a society in which hydrogen is the primary energy carrier to become realizable an efficient way of storing hydrogen is required. For this purpose metal hydrides are serious candidates. Metal hydrides are formed by chemical reaction between hydrogen and metal and for the stable hydrides this is associated with release of heat (ΔH_f). The more thermodynamically stable the hydride, the larger ΔH_f, and the higher temperature is needed in order to desorb hydrogen (reverse reaction) and vice versa. For practical application the temperature needed for desorption should not be too high i.e. ΔH_f should not be too large. If hydrogen desorption is to be possible below 100 °C (which is the ultimate goal if hydrogen storage in metal hydrides should be used in conjunction with a PEM fuel cell), ΔH_f should not exceed -48 kJ/mol. Until recently only intermetallic metal hydrides with a storage capacity less than 2 wt.% H_2 have met this criterion. However, discovering reversible hydrogen storage in complex metal hydrides such as $NaAlH_4$ (5.5 wt. % reversible hydrogen capacity) have revealed a new group of potential candiates. However, still many combination of elements from the periodic table are yet to be explored. Since experimental determination of thermodynamic properties of the vast combinations of elements is tedious it may be advantagous to have a predictive tool for this task. In this report different ways of predicting ΔH_f for binary and ternary metal hydrides are reviewed. Main focus will be on how well these methods perform numerically i.e. how well experimental results are resembled by the model. The theoretical background of the different methods is only briefly reviewed.

Descriptors

Hydrogen storage, Metal hydrides, Thermodynamics, Born-Haber cycle, Miedema model, Effective Medium Theory, Density Functional Theory, Rule of reversed stability, Binary hydrides, Complex hydrides, Magnsium based hydrides

Available on request from:
Information Service Department, Risø National Laboratory
(Afdelingen for Informationsservice, Forskningscenter Risø)
P.O. Box 49, DK–4000 Roskilde, Denmark
Phone (+45) 46 77 46 77, ext. 4004/4005 · Fax (+45) 46 77 40 13
E-mail: risoe@risoe.dk